

Surface Chemistry and Catalytic Activity of $\text{La}_{1-y}\text{M}_y\text{CoO}_3$ Perovskite (M = Sr or Th)

2. Hydrogenation of CO_2

M. A. ULLA, R. A. MIGONE, J. O. PETUNCHI, AND E. A. LOMBARDO¹

Instituto de Investigaciones en Catálisis y Petroquímica (INCAPE), Universidad Nacional del Litoral, Consejo Nacional de Investigaciones Científicas y Técnicas, Santiago del Estero 2654, 3000 Sante Fe, Argentina

Received November 1985; revised December 8, 1986

The partial substitution of La^{III} by either Sr^{II} or Th^{IV} in lanthanum cobaltate perovskite affects both the rate of hydrogenation of carbon dioxide and the distribution of products. The reaction of cyclopropane with hydrogen was used as a parallel test reaction in order to ascertain the nature of the active sites developed on these solids upon reduction. The active site density was calculated from the measured amount of chemisorbed hydrogen at 25°C on the oxides reduced at temperatures between 250 and 500°C. The catalytic activity was measured in a standard recirculation system using a $\text{H}_2:\text{CO}_2 = 4:1$ ratio, total pressure of 160 Torr, and 280°C reaction temperature. The total conversion of CO_2 into products (activity) on LaCoO_3 is little affected by the extent of reduction of the sample. More sensitive to this parameter are both the rate of methanation and the production of C_2^+ compounds. Reduced $\text{La}_{0.8}\text{Th}_{0.2}\text{CoO}_3$ is very stable giving a constant activity, the highest of all the solids assayed and almost exclusively producing methane. $\text{La}_{0.6}\text{Sr}_{0.4}\text{CoO}_3$ shows a sharp maximum in activity and high selectivity to methane when prerduced at 300°C. However, when reduced at increasing temperatures the overall activity sharply drops while the selectivity to higher hydrocarbons increases very rapidly. In all cases the unreduced solids present induction periods, which indicate that the oxide is being reduced *in situ* by the reacting mixture. In runs designed to measure the extent of deactivation due to coke deposition it was found that the degree of activity decay was inversely correlated with the methanation selectivity. The test reaction was conducted in the same system at $\text{H}_2:\text{cyclopropane} = 1:1$ ratio, $P = 170$ Torr, and 250°C. The overall activity and the product distribution toward isomerization, hydrogenation, and hydrogenolysis is very sensitive to both the nature of the solid involved and the extent of reduction. The initial rate of formation of hydrogenation plus hydrogenolysis products when plotted vs extent of reduction produces curves which are similar to those observed in methanation activity. To gain further insight into both the matrix and promoter effect a series of catalysts were prepared containing different combinations of Co, Sr, La, and Th supported on either celite or La_2O_3 . The matrix effect is most important in the Sr-substituted oxide, less so in LaCoO_3 , and unimportant in the Th-containing perovskite. The promoter effect for C_2^+ production follows the order $\text{Sr} > \text{La} \gg \text{Th}$. This and previous studies made on crystalline mixed oxides, together with data available in the literature, allowed us to propose a model to interpret the effect of lanthanum replacement upon the catalytic activity, selectivity, and stability of these solids. © 1987 Academic Press, Inc.

INTRODUCTION

Although the reaction between carbon dioxide and hydrogen is a potential source of higher valued organic compounds this has not been as extensively studied as should be expected. Among this relative paucity of in-

formation is the important effect of the support upon both the dispersion and the stability of the Group VIII metals, which in turn affect the activity and selectivity of the catalyst (1-4).

Although the effect of different promoters on the product distribution obtained during $\text{CO} + \text{H}_2$ reaction has been frequently reported, no systematic study of

¹ To whom all correspondence should be addressed.

this kind exists for the hydrogenation of carbon dioxide. The crystalline structure of perovskite oxides with its capability to accommodate many different cations affords an interesting frame of reference to test the effect of several promoters upon the catalytic behavior of the active element. In previous studies LaCoO_3 has been thoroughly characterized, the effect of hydrogen reduction upon its catalytic activity explored (5, 6), and a correlation between its surface composition and catalytic properties developed (7). Besides, in Part 1 of this study (8) the reduction process of lanthanum cobaltates partially substituted by either Th or Sr has been carefully characterized. Since, upon reduction, Co^0 appears on the surface of all these solids, "metal on oxide" catalysts can be produced either *in situ* or during the activation stage.

The work reported here was set up with the goal of investigating the effect of partial replacement of La by either Sr^{II} or Th^{IV} ($\text{La}_{1-y}\text{M}_y\text{CoO}_3$), upon the catalytic activity for hydrogenation of carbon dioxide. Furthermore, the reaction of cyclopropane with hydrogen was used as a test which could provide additional clues about the nature of the active sites which develop on the surface of these oxides upon reduction.

EXPERIMENTAL

Catalyst preparation and pretreatment. The preparation of the crystalline mixed oxides used in this study has been described in Part 1 (8). Besides, a series of supported catalysts were prepared using the following two methods: (a) incipient wetness impregnation using aqueous solution of the corresponding nitrates of Co, Sr, Th; (b) coprecipitation at a given pH from a solution containing the nitrates of pairs of elements, Co-Sr and Co-Th (9, 10). The support used in all cases but two was a celite (Kieselguhr) having a surface area of $17 \text{ m}^2/\text{g}$. In the other two cases La_2O_3 ($2 \text{ m}^2/\text{g}$) was used as a support. Both supports were used as fine powders (60–80 mesh). After either impregnation or precipitation the

solids obtained were dried overnight at 80°C , heated in air at 250°C to decompose the nitrates, and then calcined at 400°C during 4 hr.

The standard pretreatment before each catalytic experiment or hydrogen adsorption measurement was as follows: oxidation in air for 2 h followed by evacuation for 1 h at 400°C , reduction at the desired level, and final evacuation at 400°C . A lower evacuation temperature, 300°C , was adopted for Sr-containing oxides to avoid the production of additional oxygen vacancies. This was done in a standard recirculation system in which the extent of reduction could be followed volumetrically; more details have been given elsewhere (11).

Hydrogen chemisorption measurements. Hydrogen chemisorption was performed in a standard volumetric adsorption system which was modified to include a gas recirculation loop containing a liquid nitrogen trap. In this way the solid could be reduced *in situ* before the adsorption measurements. The samples were pretreated as described above. The extent of reduction was calculated from the measured hydrogen uptake.

The hydrogen adsorption isotherms were obtained at 25°C . The amount of chemisorbed hydrogen on a given sample was calculated by difference between two successive isotherms. Between them the solid was evacuated at 25°C until a vacuum better than 10^{-5} Torr was reached.

Reaction procedure. The catalytic experiments were done in the same recirculation system used for reduction into which a bulb, containing most of the reaction volume (430 cm^3), was incorporated through a bypass. The gas chromatographic (GC) analytical system was modified according to the reaction studied. When the reactants were $\text{CO}_2 + \text{H}_2$, two parallel columns of porapak R were used. One of them was held at 0°C using a TCD detector to analyze CO, CO_2 , and CH_4 . The other column was temperature programmed, from 54 to 140°C at $8^\circ\text{C}/\text{min}$, and connected to an FID detec-

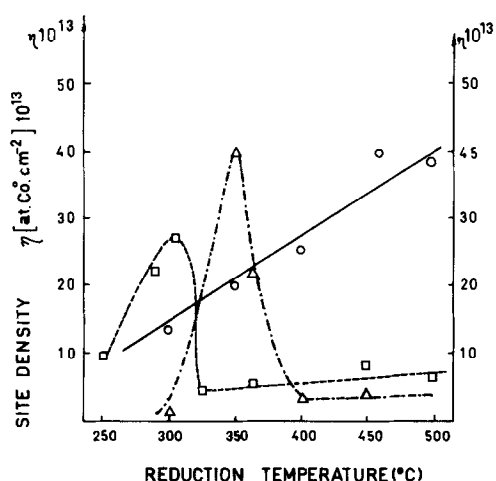


FIG. 1. The variation of surface Co⁰ with reduction temperature, calculated from the amount of H₂ chemisorbed at 25°C, assuming Co:H = 1:1. $\eta = 1.7924 \cdot 10^{15} \Delta v [\text{cm}^3 \text{ STP H}_2] / S [\text{m}^2/\text{g}]$. (Δ) LaCoO₃; (\circ) La_{0.8}Th_{0.2}CoO₃; (\square) La_{0.6}Sr_{0.4}CoO₃.

tor in order to analyze the hydrocarbons obtained. A simpler chromatographic setup was used when cyclopropane was reacted with hydrogen. In such a case a single poracil C column thermostated at 0°C connected to a TCD detector was used.

The reactant mixtures were prepared volumetrically by introducing first a measured amount of either CO₂ or cyclopropane into the recirculation system where it was frozen and outgassed before hydrogen was admitted. The reactants were thoroughly mixed before contacting the catalyst.

To evaluate the extent of deactivation of the catalyst due to coke deposition after CO₂ + H₂ reactions, a standard procedure was followed: after a 2-h-long kinetic experiment the reaction system was evacuated at room temperature for 15 min and then a new load of reactants was admitted into the system to repeat the catalytic measurement.

RESULTS

Adsorption Measurements

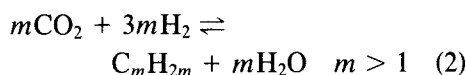
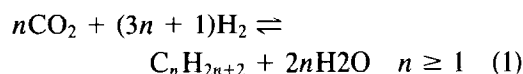
Figure 1 shows the variation in site density (η) with reduction temperatures between 250 and 500°C on three different

mixed oxides. Both the LaCoO₃ and the La_{0.6}Sr_{0.4}CoO₃ show sharp maxima in the concentration of exposed Co⁰. In fact, at reduction temperatures not far from the maxima the amounts of chemisorbed hydrogen were close to the experimental error. On the other hand, La_{0.8}Th_{0.2}CoO₃ shows a steady increase of the site density with reduction temperature.

The site density was calculated from the measured amount of chemisorbed hydrogen assuming a one to one stoichiometry (12). In a previous study CO was used with the same purpose on LaCoO₃ (5). The shape of the curve obtained was very much the same as the one shown in Fig. 1. The maximum site density calculated at 350°C was, however, only one-half of that obtained with hydrogen. Due to the uncertainty of the CO stoichiometry, 0.4 to 2.3 (12), it is not a surprise to find such a difference between the values obtained with either CO or H₂.

CO₂ + H₂ Reactions

Under the operating conditions used in this study the following equations may represent the set of reactions occurring in this system:



The experiments were conducted at 280°C, total pressure 160 Torr, and $P_{\text{H}_2}^0 / P_{\text{CO}_2}^0 = 4$.

The following parameters were defined to characterize the catalytic behavior of the system:

v^0 , initial reaction rate (mmol of CO₂ converted · m⁻² · min⁻¹)

$v_{\text{CH}_4}^0$, initial methanation rate (mmol of CH₄ · m⁻² · min⁻¹)

N_j , turnover number (TON) (molecules of j converted or produced · sec⁻¹ · site⁻¹).

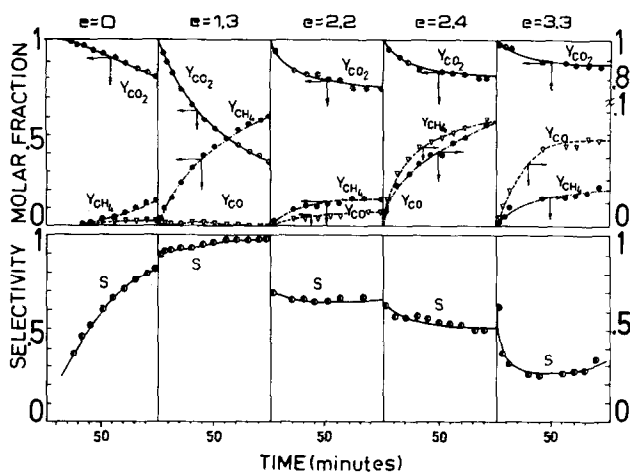


FIG. 2. $\text{CO}_2 + \text{H}_2$ reaction on LaCoO_3 , oxidized ($e = 0$) and reduced at various temperatures: $e = 1.2$ (300°C), $e = 1.3$ (350°C), $e = 2.4$ (450°C), $e = 3.0$ (500°C). Recirculation system: $\text{H}_2:\text{CO}_2 = 4:1$; temperature; 280°C ; total pressure: 160 Torr; 300 mg of catalyst. e , extent of reduction.

S_M , selectivity to methane formation [$n_{\text{CH}_4}/(n_{\text{CH}_4} + n_{\text{CO}})$].

S_X , selectivity to methane, S_M , at constant conversion of CO_2 .

Y_i , molar fraction of $i = \text{CH}_4, \text{CO}_2, \text{CO}$, not taking into account the amount of H_2O , H_2 , and hydrocarbons other than CH_4 .

C_2^+ , mass percentage of hydrocarbons containing two, three, or four carbon atoms ($100 \times m_{C_2^+}/(m_{C_2^+} + m_{\text{CH}_4})$), at constant CO_2 conversion. No higher molecular weight

hydrocarbons were detected through the FID.

Figures 2–4 show the results obtained with three different perovskites. In Table 1 the main features of the catalytic experiments are summarized to facilitate the comparison among the various oxides.

LaCoO_3 . The initial reaction rate (v^0) of the reduced oxide fluctuates with extent of reduction (Table 1), but it does not show a maximum as was the case for hydrogenation

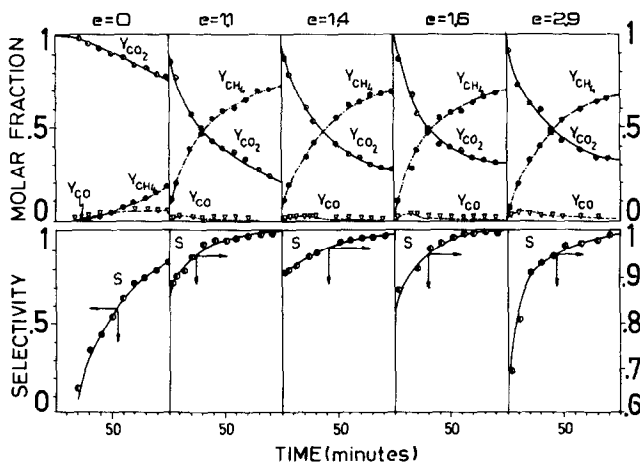


FIG. 3. $\text{CO}_2 + \text{H}_2$ reaction on $\text{La}_{0.8}\text{Th}_{0.2}\text{CoO}_3$, oxidized ($e = 0$) and reduced at various temperatures: $e = 1.1$ (300°C), $e = 1.4$ (350°C), $e = 1.6$ (400°C), $e = 2.9$ (500°C). For reaction conditions see Fig. 2.

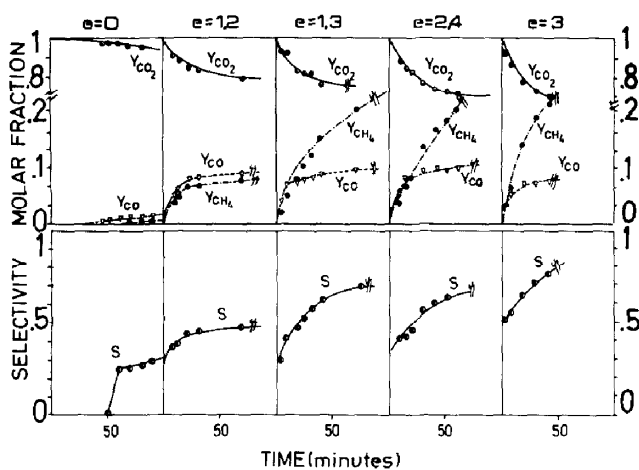


FIG. 4. CO₂ + H₂ reaction on La_{0.6}Sr_{0.4}CoO₃, oxidized ($e = 0$) and reduced at various temperatures: $e = 1.3$ (300°C), $e = 2.2$ (350°C), $e = 2.4$ (400°C), $e = 3.3$ (500°C). For reaction conditions see Fig. 2.

TABLE I

CO₂ + H₂ Reaction over La_{1-y}M_yCoO₃ (M = Sr, Th): Catalytic Activity Selectivity and C₂⁺ Production at Different Extents of Reduction^a

Perovskite	Reduction temperature (°C)	Extent of reduction ^b (e^-/molec)	$v^0 \times 10^3$	S_X^c	C ₂ ⁺ ^d
LaCoO ₃	—	0.0	^e	0.65	0
	300	1.2	10.4	0.52	13
	350	1.3	20.2	0.54	11
	400	1.4	20.7	0.57	6
	450	2.4	13.7	0.58	4
La _{0.8} Th _{0.2} CoO ₃	—	0.0	^e	0.70	0
	300	1.1	130	0.89	2
	350	1.4	123	0.92	2
	400	1.6	130	0.87	2
La _{0.6} Sr _{0.4} CoO ₃	—	0.0	^e	0.80	0
	300	1.3	40	0.91	3
	350	2.2	14.7	0.67	18
	400	2.4	14.4	0.55	14
	500	3.3	4.2	0.32	30

^a Batch gas recirculating system, H₂:CO₂ = 4.1; reaction temperature 280°C, total pressure 160 Torr; 300 mg of catalyst.

^b Reduction of Coⁿ⁺ to Co⁰ corresponds to n electrons per formula weight of mixed oxide.

^c Selectivity to methane at constant CO₂ conversion $X_{\text{CO}_2} = 0.20$.

^d The C₂⁺ fraction included hydrocarbons containing two, three and four carbon atoms; at constant CO₂ conversion $X_{\text{CO}_2} = 0.20$.

^e The reaction showed an induction period.

of either ethylene (5) or cyclopropane (Fig. 5). The production of C_2^+ products decreases at higher reduction levels, while the selectivity toward methane production, measured at the same CO_2 conversion, follows the opposite trend (Table 1). It is also noted that S_M increases as the reaction proceeds, an effect which is even more pronounced at the highest extent of reduction (Fig. 2). The concentration of carbon monoxide shows a similar behavior for all the reduced samples, reaching a plateau value between 0.08 and 0.1 (Fig. 2). The oxidized sample shows a long induction period and then the reaction proceeds slowly.

$La_{0.8}Th_{0.2}CoO_3$. This solid is much more active and selective to methane than $LaCoO_3$. The extent of reduction does not affect the initial rate and C_2^+ is very low (Table 1). The selectivity increases up to 99% along the reaction time for all the reduced samples, while the Y_{CO} curve shows a flat maximum and then decreases to zero (Fig. 3). The oxidized solid shows a shorter induction period, and then becomes more active than $LaCoO_3$ (compare Figs. 2 and 3).

$La_{0.6}Sr_{0.4}CoO_3$. This oxide has two completely different behaviors as can be observed in Fig. 4. When the solid has not been reduced or treated with hydrogen at 300°C, the product distribution obtained was very close to that shown by the Th-substituted specimen. When reduced at higher temperatures it shows a behavior which is completely different from those of the other oxides; e.g., the selectivity to methane decreases and the C_2^+ product increases with extent of reduction. Particularly, the most reduced sample gave the highest selectivity to C_2^+ products of all the formulations assayed (Table 1).

Deactivation by Coke Formation

In Table 2 the results are shown of a pair of experiments designed to evaluate the extent of deactivation under standard conditions of four different oxides. To detect the presence or coke (residues) on the catalyst, this was heated in oxygen at 400°C in the

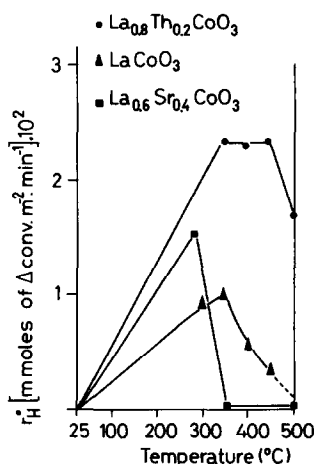


FIG. 5. Hydrogenation and hydrogenolysis of cyclopropane (Δ) over $La_{1-y}M_yCoO_3$. Recirculation system; H_2 : Δ = 1 : 1, temperature: 250°C; total pressure: 170 Torr, 300 mg of catalyst. r_H^0 , initial rate of Δ hydrogenation and hydrogenolysis.

recirculation system after the reaction and the gas phase was analyzed with the on-line gas chromatograph. The oxides containing Th were the less affected by coke formation. Both $LaCoO_3$ and the oxide containing Sr suffered strong deactivation, showing at the same time an increased activity to produce C_2^+ hydrocarbons. The Sr oxide was also assayed at maximum reduction due to its high sensitivity to this parameter (Table 2).

A general trend emerges from these observations: the higher the production of C_2^+ the more sensitive to deactivation becomes the catalyst. This holds true in all cases.

Supported Cobalt

In order to ascertain the role of the perovskite matrix on the promoting effect of La, Th, and Sr, a series of cobalt-supported catalysts was tried (Table 3). The parameters chosen from this purpose were S_X and C_2^+ . The Co/celite system was considered to represent the behavior of unpromoted metallic cobalt.

Cyclopropane (Δ) + H_2 Reactions

At 250°C the following reactions can be catalyzed by reduced mixed oxides:

TABLE 2
Deactivation by Coke Formation^a

Perovskite	Reduction temperature (°C)	Extent of reduction (e ⁻ /molec)	$\nu_{\text{CH}_4}^0 \cdot 10^{3b}$	S_X^c	C_2^{+d}
LaCoO ₃	350	1.3	4.5 ^e	0.54	13
			<i>f,g</i>	0.32	30
La _{0.8} Th _{0.2} CoO ₃	300	1.1	110.5 ^e	0.88	2
			80.1 ^f	0.86	2
La _{0.9} Th _{0.1} CoO ₃	350	0.7	28.6 ^e	0.75	4
			7.1 ^f	0.46	7
La _{0.6} Sr _{0.4} CoO ₃	350	2.1	10 ^e	0.65	18
			<i>f,g</i>	0.32	45
La _{0.6} Sr _{0.4} CoO ₃	500	3.3	2.5 ^e	0.32	30
			<i>f,h</i>	0.15	50

^a Recirculation system, H₂:CO₂ = 4:1; reaction temperature 280°C, total pressure: 160 Torr; 300 mg. catalyst.

^b mmol · CH₄ prod/m² · min⁻¹.

^c Selectivity at conversion of CO₂, X_{CO₂} = 0.12.

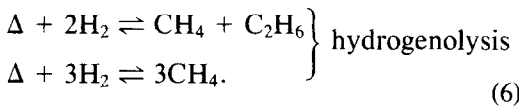
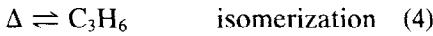
^d C₂⁺ at 30 min reaction time.

^e The catalyst was given the standard pretreatment.

^f These experiments were done after evacuation of the catalyst at room temperature for 15 min, following the previous run.

^g The reaction showed an induction period.

^h The first product to appear was CO.



The experiments were run at a total pressure of 170 Torr and $P_{\text{H}_2}^0/P_{\Delta}^0 = 1$.

The following parameters were defined to characterize the reacting system:

r^0 , initial rate of Δ consumption (mmol of cyclopropane converted · m⁻² · min⁻¹).

r_{H}^0 , initial rate of Δ hydrogenation and hydrogenolysis, same units as r^0 .

S_{H}^0 , initial selectivity toward hydrogenolysis:

$$\frac{\frac{1}{3}(n_{\text{CH}_4} - n_{\text{C}_2\text{H}_6}) + n_{\text{C}_2\text{H}_6}}{\frac{1}{3}(n_{\text{CH}_4} - n_{\text{C}_2\text{H}_6}) + n_{\text{C}_2\text{H}_6} + n_{\text{C}_3\text{H}_8}}$$

S_I^0 , initial isomerization selectivity:

$$\frac{n_{\text{C}_3\text{H}_6}}{n_{\text{C}_3\text{H}_6} + \frac{1}{3}(n_{\text{CH}_4} - n_{\text{C}_2\text{H}_6}) + n_{\text{C}_2\text{H}_6}}$$

TABLE 3

Methanation Selectivity and C₂⁻ Production of Supported Co^a

Catalyst	S_X^b	C_2^{+c}	S_M^d
LaCoO ₃	0.56	11	0.50
5%Co/Celite ^e	0.78	6	0.93
5%Co/La ₂ O ₃ ^e	0.46	14	0.36
La _{0.8} Th _{0.2} CoO ₃	0.91	2	0.95
5%Co.5%Th/celite ^f	0.76	2	0.90
5%Co/5%Th/celite ^g	0.86	2	0.90
La _{0.6} Sr _{0.4} CoO ₃	0.67	18	0.70
5%Co.5%Sr/celite ^f	0.51	6	0.30
5%Co/5%Sr/celite ^h	0.63	6	0.83
5%Co/5%Sr/La ₂ O ₃ ^g	0.46	11	0.50

^a See reaction conditions in Table 1. All the solids were pretreated in H₂ at 350°C.

^b Selectivity to methane at X_{CO₂} = 0.20.

^c Measured at constant CO₂ conversion, X_{CO₂} = 0.20.

^d Selectivity to methane at 30 min reaction time.

^e Incipient wetness impregnation.

^f Coprecipitated at a controlled pH.

^g Either the Th or Sr was impregnated first and then the Co on top.

TABLE 4
Catalytic Activity and Selectivity of Reduced Mixed Oxides for
Cyclopropane plus Hydrogen Reaction^a

Perovskite	Reduction temperature (°C)	Extent of reduction (e ⁻ /molec)	$r^0 \times 10^{3b}$	S_H^{0c}	S_I^{0c}
LaCoO ₃	300	0.9	9.2	0.90	0
	350	1.1	9.8	0.80	0
	400	1.2	5.6	0.85	0
	450	2.5	3.9	0.60	0
La _{0.8} Th _{0.2} CoO ₃	350	1.2	23.1	0.90	0
	400	1.7	22.9	0.90	0
	450	2.9	23.1	0.90	0
	500	2.9	16.7	0.90	0
La _{0.6} Sr _{0.4} CoO ₂	280	1.3	15.3	0.81	0
	350	2.0	8.8	0.0	1
	500	3.2	0.2	0.3	0
La _{0.4} Sr _{0.6} CoO ₃	350	2.8	^d	0.0	1
	500	3.3	0.01	0.01	0

^a Recirculation system, H₂:C₃H₆ = 1:1; temperature: 20°C; total pressure: 170 Torr; 300 mg of catalyst.

^b Initial reaction rate of Δ consumption (mmole of Δ converted · m⁻² min⁻¹).

^c Initial selectivity toward hydrogenolysis (S_H^0) and isomerization (S_I^0).

^d The reaction showed an induction period.

Figure 5 shows the effect of reduction upon both the hydrogenation and hydrogenolysis activity of three mixed oxide formulations. Note that the initial reaction rates (r_H^0) plotted in Fig. 5 take into account the hydrogenation and hydrogenolysis products, but do not include the rate of isomerization.

The Sr-substituted solid shows a sharp drop in activity at reduction temperatures higher than 300°C. Besides, it should be noted the singular behavior of this oxide when reduced at 350°C, where the hydrogenolysis activity falls to zero, the hydrogenation rate is extremely low, while the isomerization product is predominant (Table 4). This behavior was further checked in the case of another sample containing a higher proportion of Sr, La_{0.4}Sr_{0.6}CoO₃ (Table 4).

The LaCoO₃ also shows a maximum in activity although much less pronounced (Fig. 5). At the same time the selectivity is

less affected and no propylene was concerned in the gas phase at any reduction temperature (Table 4).

The most stable oxide is again the one partially substituted by Th. The selectivity to hydrogenolysis is not affected by high reduction temperatures (Table 4), while the initial rate (r^0) somewhat decreases after reduction at 500°C.

Specific Activities of Reduced Mixed Oxides

Table 5 shows that N_{CO_2} , N_{CH_4} and N_{Δ} decrease at higher extents of reduction of La_{0.8}Th_{0.2}CoO₃, despite the fact that the site density (η) increases in this direction (Fig. 1). On the other hand, the TON variation seems to correlate with the Co/Th surface atomic ratio measured by XPS (Fig. 11, Part 1). This may indicate that a good contact between neighboring Co-Th atoms is a key factor to obtain high-specific hydrogenation activity.

TABLE 5

Effect of the Reduction Temperature upon the Specific Activity and Selectivity of La_{0.8}Th_{0.2}CoO₃^a

Reduction temperature (°C)	Extent of reduction (e ⁻ /molec)	N _Δ × 10 ^{3b} (s ⁻¹)	N _{CO₂} × 10 ^{3c} (s ⁻¹)	N _{CH₄} × 10 ³ (s ⁻¹)	S _X ^d	Co/Th ^e
300	1.1	—	971	855	0.89	3.2
350	1.4	115	618	556	0.92	6.5
400	1.6	90	502	427	0.82	7.7
500	2.9	41	287	194	0.80	10.0

^a Reaction conditions see Tables 1 and 4.^b N_Δ, molecules of cyclopropane converted per second and per active site.^c N_{CO₂} and N_{CH₄} are given for comparison because CO₂ may be converted to CO in nonmetallic sites.^d Measured at X_{CO₂} = 0.20.^e Values of atomic ratio from Fig. 11, Part 1.

It is interesting to now compare the TON values for the three mixed oxides when reduced at the same extent (1.3 e⁻/molecule). The specific activity is strongly affected by the cation accompanying the Co in the mixed oxide (Table 6). On the selectivity side, the Sr- and Th-containing oxides behave very much the same, but the LaCoO₃ shows a different product distribution.

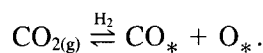
DISCUSSION

In Part 1 of this series the reduction process of these oxides was modeled (8). A common feature observed after the hydrogen treatment followed by evacuation of both LaCoO₃ and La_{0.6}Sr_{0.4}CoO₃ is the appearance of a maximum in the Co⁰ surface concentration when plotted as a function of the reduction temperature. On the other hand, the La_{0.8}Th_{0.2}CoO₃ does not show

this behavior; the Co⁰ surface concentration steadily increases with higher reduction temperatures. The hydrogen chemisorption data shown in Fig. 1 further confirm this behavior.

Before discussing the catalytic properties of each oxide it is useful to point out a few well-established characteristics of the hydrogenation of CO₂ and cyclopropane.

It is widely accepted that CO₂ is dissociatively adsorbed in the presence of hydrogen over most Group VIII metals (1, 3, 4, 13, 14).



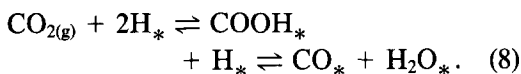
Alternatively, a formate group has been detected by IR on the oxide support (15–17). This group could in turn be another sort of intermediate for CO production.

TABLE 6

Turnover Numbers and Selectivities of Several Perovskites at a Constant Extent of Reduction^a

Perovskite	Reduction temperature (°C)	Extent of reduction (e ⁻ /molec)	N _Δ × 10 ³ (s ⁻¹)	N _{CO₂} × 10 ³ (s ⁻¹)	N _{CH₄} × 10 ³ (s ⁻¹)	S _X	C ₂ [†]
LaCoO ₃	350	1.3	25	50	15	0.54	11
La _{0.8} Th _{0.2} CoO ₃	350	1.4	115	618	556	0.92	2
La _{0.6} Sr _{0.4} CoO ₃	300	1.3	67	182	164	0.91	3

^a Reaction conditions see Tables 1 and 4. Symbols see Table 5.



It is also well known (1-4, 13, 18-26) that an essential step leading to hydrocarbon synthesis is the dissociation of the CO_* to produce an active surface carbon C_* which would be the key to achieve a high catalytic activity:



Cyclopropane, in the presence of hydrogen, may react to give C_3H_6 (isomerization), C_3H_8 (hydrogenation), and $\text{C}_2\text{H}_6 + \text{CH}_4$ (hydrogenolysis). The predominance of each of these reactions is a function of the surface properties of the catalyst. Over basic oxides (e.g., SrO) the main product is the olefin accompanied by small amounts of propane, over transition metal oxides the hydrogenation product is almost exclusively produced, while transition metals catalyze both the hydrogenation and hydrogenolysis reactions. This is why this reaction system was chosen as a probe to ascertain the nature of the active sites operating on these oxides.

LaCoO₃

Both the rate of methanation and the C_2^+ production were affected by the extent of reduction (Table 1). S_X and C_2^+ show a direct correlation with the Co/La ratio which rapidly increases at reduction temperatures above 350°C, see Fig. 11 in (8); e.g., at 500°C this ratio is increased to about 9 and consequently the promoting effect of La becomes negligible.

Both the hydrogenation and hydrogenolysis of cyclopropane were more affected by the reduction level (Fig. 5). This behavior is similar to that reported for the hydrogenation of ethylene at -20°C (5). The LaCoO_3 chemisorption curve shows a maximum in the concentration of exposed Co^0 (Fig. 1) coincident with the highest activity in Fig. 5. To the right of the maximum, however, the activity curve shows a less pronounced decrease than the chemisorption capacity.

This may be due to the removal of the cobalt oxide formed on top of the Co^0 cluster (Fig. 13, Part 1 (8)) by a reducing reacting mixture at temperatures above 250°C.

Another symptom of surface rearrangement during reaction may be the shape of the Y_{CO} vs time curves (Fig. 2) which approach the same plateau value (0.08-0.1), independently of the extent of reduction. Bartholomew *et al.* (2, 19) have reported a similar behavior on supported Group VIII metals, which was interpreted as the result of reaching the equilibrium between gas phase and adsorbed carbon monoxide. This in turn could also be related with a steady-state distribution of C_* and H_* on the catalyst surface which governs the selectivity to methane and higher hydrocarbons.

La_{0.8}Th_{0.2}CoO₃

This oxide, upon reduction, shows the highest catalytic activity (Tables 1 and 4). This correlates with the ability of Th to suppress the formation of hydroxyl groups on the surface of the reduced oxide (Table 4 of Part 1), thus preventing the reoxidation of Co^0 as shown by the chemisorption measurement (Fig. 1).

The results obtained with cyclopropane point in the same direction, i.e., the constant high selectivity to hydrogenolysis products (Table 4) and the less pronounced effect of high reduction temperatures upon the activity than those observed with the other oxides (Fig. 5).

Both the methanation and cyclopropane TONs decrease and the Co/Th ratio increases as the reduction temperature goes up (Table 5). This seems to indicate that a close interaction between Th and Co enhances the specific activity. The cause of this behavior is not known at this time.

Figure 3 shows that CO behaves as an intermediate, its concentration in the gas phase being very low due to the high hydrogenation activity of this catalyst. This in turn reduces the competing chain-growing process; i.e., both the C_2^+ concentration and

the coke deactivation are much lower than in the other oxides. This is also reflected in more stable initial reaction rates (Tables 1 and 4).

La_{0.6}Sr_{0.4}CoO₃

This solid shows a sharp maximum in activity for both cyclopropane hydrogenation and CO₂ methanation upon reduction at 300°C (Table 1, Figs. 4 and 5). These results are consistent with both the reduction behavior (Part 1) and the hydrogen chemisorption results (Fig. 1). This more easily reduced solid shows the highest concentration of terminal hydroxyls after reduction (see Table 5 in Part 1). Another important feature of this oxide is the migration of Sr toward the surface which begins between 250 and 300°C (Fig. 5 in Part 1). This segregation produces a drastic change in the product distribution of the cyclopropane reaction upon reduction of the solid at 350°C. At this temperature the almost exclusive product is propylene (Table 4), meaning that the surface behaves as a basic oxide due to the presence of SrO while little if any metal is visible to the reactants (Fig. 1).

At higher reduction temperatures, $\geq 400^\circ\text{C}$, the solid becomes almost inactive for all cyclopropane reactions, in agreement with the low hydrogen chemisorption values seen in Fig. 1. To explain these results it is useful to recall again the XPS data. The O1s spectra at temperatures $\geq 400^\circ\text{C}$ only show the presence of hydroxyls; i.e., the O²⁻ signal from the lattice is completely blocked by the OH groups (Table 5 in Part 1). This overwhelming presence of basic hydroxyls on the surface explains the inability of the highly reduced solid to even isomerize cyclopropane.

A large change in both selectivity and activity was also observed when CO₂ was hydrogenated. Up to 280°C, perhaps 300°C, methane is the main product but at higher reduction levels, both the production of C₂⁺ (Table 1) and the coke deactivation effect (Table 2) sharply increase.

This effect is clearly understood in terms

of the cyclopropane test reaction which together with the XPS data (8) shows the importance of the Sr segregation in the behavior of this system. Besides, the ability of basic cations to increase the selectivity toward higher hydrocarbons is a well-known feature in Fischer-Tropsch chemistry (27).

Unreduced Mixed Oxides

When LaCoO₃ was not pretreated with H₂ a long induction period was observed during which the solid was reduced (Fig. 2). As expected, the first reaction product was CO which was probably formed on the Co²⁺ sites by the inverse water gas shift reaction (4, 17, 28, 29). Later, CH₄ is formed and this could be related to the appearance of Co⁰ on the surface. It should be remembered that at this low-temperature reduction is likely to proceed stepwise according to the data shown by Sis *et al.* (30), Crespin and Hall (31), and in Part 1.

From Figs. 2–4 it is concluded that both the Th- and Sr-containing oxides are activated much more rapidly *in situ* than LaCoO₃. To explain these results one looks first at Fig. 1 of this work and Fig. 6 in Part 1. It is seen in both figures that the Co⁰ concentration on the surface at 280–300°C decreases in the order Sr > Th > LaCoO₃. Now turning to Tables 5 and 6, they show that n_{CH_4} decreases in the direction Th > Sr \gg LaCoO₃. Combining these two observations it is understandable that the induction periods will be of about the same length for both the Th- and Sr-containing oxides and much longer for the lanthanum cobaltate. Also note that the presence of water vapor does not affect the *in situ* reduction at 280°C as expected from the XPS measurements made under similar conditions (8).

Matrix and Promoter Effect

Most evidences indicate that the main component of the active sites is the metallic cobalt which appears on the surface of these oxides upon reduction. The question is how the specific activity of these sites is affected by the surrounding matrix. Table 6

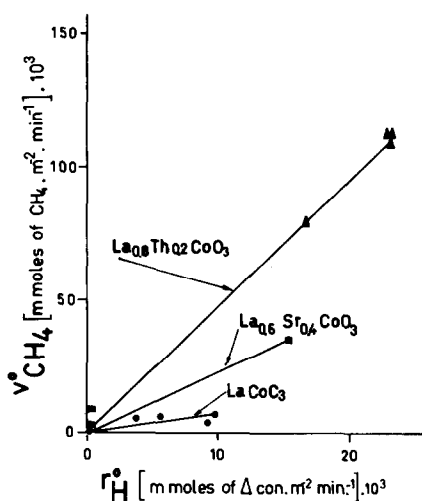


FIG. 6. Relationship between initial rates of methanation of CO_2 ($v_{\text{CH}_4}^0$) and hydrogenation of cyclopropane (r_{H}^0) over reduced $\text{La}_{1-y}\text{M}_y\text{CoO}_3$.

gives an answer to this matter. Both N_{CH_4} and N_{Δ} are affected by the matrix, but this effect is more pronounced in the methanation reaction. At the same bulk reduction level the Th-containing oxide is more active than the Sr-containing oxide but their selectivities are the same. However, at higher reduction temperatures the catalytic behavior of these oxides are completely different. Table 6 also shows that LaCoO_3 is the less active of the three solids, while at increasing reduction temperatures both S_X and C_2^+ approach the values obtained with the Th-substituted oxide (Table 1).

Weatherbee and Bartholomew (18) have reported N_{CH_4} values for silica-supported cobalt catalysts. They obtained the data using a flow reactor and a 4:1 = H_2 : CO_2 reactant ratio. At 550 K and 53 Torr total reactant pressure they reported $N_{\text{CH}_4} = 10.2$ for a $\text{Co}(3\%)/\text{SiO}_2$. From their data we have also calculated a value of $N_{\text{CH}_4} = 232$ at 550 K and 760 Torr for a $\text{Co}(15\%)/\text{SiO}_2$ catalyst. Comparing these results with those of Table 6, it is concluded that the metallic cobalt present on both the Sr- and Th-containing oxides has a higher specific methanation activity than Co on silica.

Figure 6 further confirms the matrix effect. The experimental points fall, with one exception, in three straight lines, each one corresponding to a different oxide. The slopes of these lines decrease in the same direction as N_{CH_4} in Table 6.

One last question remains to be answered. Up to what extent is the effect of the promoters, La-Sr-Th, associated with the perovskite structure. Table 3 throws some light onto this problem.

Comparing the data reported in the first three rows, it seems that the effect of La on both S_M and C_2^+ is independent of the way this element is incorporated into the catalyst. In fact, if additional data are taken into account it is concluded that the factor controlling the selectivity is the Co/La ratio. Combining the results of Fig. 11 in Part 1 with Table 1 here it is seen that S_X goes up and C_2^+ goes down when the Co/La ratio increases from 1 to 10. The $\text{Co}(5\%)/\text{La}_2\text{O}_3$ sample shows by XPS a Co/La ratio of 0.5 (32) and fits into this series. Thus, the perovskite structure affords a possible route to control the selectivity of the catalyst through an appropriate hydrogen pretreatment.

Lines 4 to 6 in Tables 3 and 5 make clear that the Co/Th ratio only affects the specific activity of the system but not the selectivity of the Th-Co system. The effect of lanthanum is completely blocked by the presence of thorium.

Table 3 finally shows that in the case of Sr there is a marked difference in catalytic behavior according to the way this element is added. It seems that a matrix such as the perovskite which permits a high dispersion of the elements in the starting material is essential to obtain a high selectivity toward the production of C_2^+ , which can even be enhanced by a suitable hydrogen pretreatment (Table 1).

CONCLUSIONS

The effect of hydrogen treatment on the surface structure of these solids has been sketched in Fig. 13 in Part 1, based upon

the XPS measurements. The hydrogen chemisorption and catalytic data reported here lend further support to the model.

Co⁰ is a necessary component of the active site but its specific activity and selectivity is strongly influenced by the accompanying cations i.e.,

The drastic changes in turnover numbers effected by the different cations.

The role played by the high dispersion of the components in the crystalline catalyst precursor in determining the catalytic properties of the reduced solids (matrix effect).

The cobalt/cation surface ratios which are modified by the hydrogen treatment produce sharp changes in both TON and selectivity.

The selectivity toward C₂⁺ production when CO₂ is hydrogenated is affected by the promoters in the same way as in the case of carbon monoxide, i.e., Sr > La ≫ Th. This seems to indicate that both reactions start from the same point, CO, in agreement with other authors (1, 3, 4, 20, 24, 26).

ACKNOWLEDGMENTS

We are indebted to the Japan International Cooperation Agency for the donation of an ESCA 750 Shimadzu spectrometer. This work was supported by grants from CONICET and SECYT.

REFERENCES

1. Iizuka, T., Tanaka, Y., and Tanabe, K., *J. Catal.* **76**, 1 (1982).
2. Weatherbee, G. D., and Bartholomew, C. H., *J. Catal.* **63**, 67 (1981).
3. Erdhoelyi, A., Kocsig, M., Banasagi, T., and Solymosi, F., *Acta Chim. Acad. Sci. Hungaricae, Tomus* **111**(4), 591 (1982).
4. Rofer-De Poorter, C. K., *Chem. Rev.* **81**, 447 (1981).
5. Petunchi, J. O., Ulla, M. A., Marcos, J. A., and Lombardo, E. A., *J. Catal.* **70**, 356 (1981).
6. Nudel, J. N., Umansky, B. S., Piagentini, R. O., and Lombardo, E. A., *J. Catal.* **89**, 362 (1984).
7. Lombardo, E. A., Tanaka, K., and Toyoshima, I., *J. Catal.* **80**, 340 (1983).
8. Marcos, J. A., Buitrago, R. H., and Lombardo, E. A., *J. Catal.* **105**, 95-106 (1987).
9. Bartholomew, C. H., and Pannell, R. B., *J. Catal.* **65**, 390 (1980).
10. Pennline, H. W., Gornley, R. J., and Schell, R., *Ind. Eng. Chem. Prod. Res. Dev.* **23**, 388 (1984).
11. Ulla, M. A., Miro, E. E., and Lombardo, E. A., in "Proceedings, 8th Iberoamerican Symposium on Catalysis," p. 745 (1982).
12. Reuel, R., and Bartholomew, C. H., *J. Catal.* **85**, 63 (1984).
13. Falconer, J. L., and Zagli, A. E., *J. Catal.* **62**, 280 (1980).
14. Henderson, M. A., and Worley, S. D., *Surf. Sci. Lett.* **149**, L1 (1985).
15. Solymosi, F., Erdohelyi, A., and Kocsis, M., *J. Catal.* **65**, 428 (1980).
16. Solymosi, F., Bansagi, T., and Erdohelyi, A., *J. Catal.* **72**, 166 (1981).
17. Amenomiya, Y., *J. Catal.* **57**, 64 (1979).
18. Weatherbee, G. D., and Bartholomew, C. H., *J. Catal.* **87**, 352 (1984).
19. Vance, K. C., and Bartholomew, C. H., *Appl. Catal.* **7**, 169 (1983).
20. Weatherbee, G. D., and Bartholomew, C. H., *J. Catal.* **77**, 460 (1982).
21. Araki, M., and Ponec, V., *J. Catal.* **44**, 439 (1976).
22. Biloen, P., Recueil, *J. R. Neth. Chem. Soc.* **99**, 33 (1980).
23. Vannice, M. A., in "Catalysis—Science and Technology" (J. R. Anderson, and M. Boudart, Eds.), Vol. 3, Chap. 3, p. 144. Springer-Verlag, Heidelberg, 1982.
24. Dalmon, J. A., and Martin, G. A., *J. Chem. Soc. Faraday Trans. I* **75**, 165 (1979).
25. Kort, J. G. E., and Bell, A. T., *J. Catal.* **58**, 170 (1979).
26. Inoue, H., and Funakoshi, M., *J. Chem. Eng. Japan* **17**(6), 602 (1984).
27. Dory, M. E., Shingles, T., Boshoff, L. J., and Oosthuizen, G. J., *J. Catal.* **15**, 190 (1969).
28. Thomson, S. J., and Webb, G., in "Heterogeneous Catalysis," p. 174. Oliver & Boyd, Edinburgh/London, 1960.
29. Grenoble, D. C., and Estadt, M. M., *J. Catal.* **67**, 90 (1981).
30. Sis, L. B., Wirtz, G. P., and Sorenson, S. C., *J. Appl. Phys.* **44**, 5553 (1973).
31. Crespin, M., and Hall, W. K., *J. Catal.* **69**, 359 (1981).
32. Nudel, J. N., Umansky, B. S., and Lombardo, E. A., *Appl. Catal.* **26**, 339 (1986).